EARTHARXIV PREPRINT — NON-PEER-REVIEWED MANUSCRIPT

Fabric memory during repeated reversal shear in clay-rich materials: An experimental study using SEM, SP-μCT, and AMS

Kiichiro Kawamura 1

1 Graduate School of Science and Technology for Innovation, Yamaguchi University, 1677-1 Yoshida, Yamaguchi-City, Yamaguchi 753-8512, Japan

* Correspondence:
Corresponding Author Kiichiro Kawamura

Preprint version 1 — 8 September 2026

kiichiro@yamaguchi-u.ac.jp

Keywords: Reversal shear; Fabric memory; Clay-rich shear zone; Fault gouge; Microfabric; Magnetic susceptibility anisotropy

Highlights

Repeated reversal shear produces a cumulative clay-rich fabric.
SEM and SP-μCT reveal particle reorganization after ten reversal cycles.
AMS records Kmax transverse to the imposed shear direction.
The final fabric is consistent with rotational gouge reorganization.
Reversal shear can preserve elements of earlier deformation.

Abstract

Fine-grained shear zones occur in both tectonic faults and gravitational landslides, making their origin difficult to determine from individual microstructural features alone. A potentially useful distinction is provided by deformation history: tectonic faults commonly experience repeated earthquake cycles in which the sense and magnitude of deformation may change, whereas landslide slip zones are primarily governed by gravitational downslope loading. How reversal of shear is recorded in clay-rich microfabric, however, remains poorly understood. Here, I investigate the development of

fabric memory during repeated reversal shear using direct-shear experiments on clay-rich materials from the Jin'nosuke-dani landslide, central Japan. Undisturbed and slurry samples were tested under normal stresses of 0.4, 0.8, and 1.6 MPa. Following 1000 min of pre-consolidation, specimens underwent ten predetermined shear cycles, with the shear direction reversed after each cycle. Shear stress and vertical displacement were recorded automatically, and the experimentally deformed materials were examined by scanning electron microscopy (SEM), synchrotron radiation micro-X-ray computed tomography (SP-μCT), and anisotropy of magnetic susceptibility (AMS).

SEM and SP-μCT reveal preferred clay-flake orientations, fragmented and locally rotated shale clasts, asymmetric structures, and three-dimensional reorganization of the clay-rich material. AMS provides a complementary bulk-scale constraint, with Kmax approximately horizontal and oriented perpendicular to the imposed shear direction. The transverse Kmax orientation, together with the observed particle and clast rotation, is consistent with rotation and rolling of gouge-like material during reversal shear. We propose that reversal does not simply erase the fabric generated during the preceding shear cycle. Instead, elements of the earlier fabric are retained while being rotated, disrupted, and overprinted by deformation in the opposite direction. Repeated reversal therefore produces a composite fabric that records cumulative deformation history, which I refer to as experimental fabric memory.

This rotational fabric memory may be associated with deformation histories involving repeated reversal and could provide a process-based line of evidence for distinguishing tectonic shear zones from gravitational landslide slip zones when combined with independent geological, geomorphological, and kinematic evidence. The present study does not establish that the observed fabric is uniquely tectonic, because the experiments were performed on landslide-derived material and the fabric was measured only after the ten-cycle test. Rather, it demonstrates a testable mechanism by which reversal deformation can leave a distinctive microfabric signature.

1. Introduction

Shear deformation produces characteristic fabrics in both tectonic fault zones and gravitational landslide slip zones. These fabrics may preserve information on the sense of movement, deformation history, and strain within a shear zone (Ramsay and Huber, 1983). In particular, preferred orientations of clay particles and other fine-grained constituents can develop during shear deformation, and their development depends on stress, strain, material properties, and deformation conditions (Moore et al., 1989).

Because both tectonic faults and landslide slip surfaces accommodate shear deformation, similar microstructures may develop in shear zones formed by fundamentally different driving mechanisms. An early comparison of a natural landslide shear zone and laboratory-sheared kaolin demonstrated that preferred particle orientations can develop in both natural and experimental shear zones and can be related to the principal stress configuration (Tchalenko, 1968). Subsequent laboratory studies of clay-rich gouges have shown that Riedel shears and preferred clay-particle orientations develop systematically during shear deformation (Haines et al., 2013). These observations demonstrate the potential of clay microfabric for reconstructing deformation processes, but also indicate that the presence of a clay-rich shear zone or a preferred mineral fabric alone does not uniquely establish whether the structure formed by tectonic faulting or gravitational sliding.

This problem is particularly important where landslides develop within rocks that have previously experienced tectonic deformation. Pre-existing tectonic fabrics may be incorporated into landslide slip zones and subsequently modified by gravitational shear. Conversely, similar clay fabrics are well documented in natural and artificial fault gouges (Haines et al., 2009). Therefore, the interpretation of clay microfabric requires comparison with independent constraints on the deformation environment, including field kinematics, shear-zone geometry, geomorphological setting, and the relationship between mineral fabric and inferred slip direction.

Magnetic fabrics can provide an additional constraint on particle preferred orientation when the magnetic susceptibility is dominated by minerals associated with the deforming matrix (Tarling and Hrouda, 1993). Previous studies have demonstrated relationships between magnetic fabrics and deformation fabrics in tectonically deformed sediments and shear zones (Rathore et al., 1983; Housen and Sato, 1995; Housen, 1997). Combining SEM observations with AMS therefore provides an opportunity to compare independently measured microstructural and magnetic fabrics.

Natural landslide slip zones provide an opportunity to investigate the development of shear fabrics under gravitational loading. Some landslides contain basal slip zones that undergo long-term creep under residual-strength conditions, and the deformation structures preserved in such zones may record the cumulative effects of repeated displacement. However, direct comparison between natural landslide fabrics and laboratory-generated fabrics is complicated by large differences in strain rate, total displacement, and boundary conditions (Mandl, 2000).
The Jin'nosuke-dani landslide is particularly relevant because its basal slip-zone fabric has previously been compared with the fabric and slip mechanism of a proto-décollement in an accretionary prism (Kawamura et al., 2007). That comparison showed that clay-rich shear fabrics developed under gravitational sliding can resemble those associated with tectonic shear. The present study takes this comparison one step further by isolating reversal of shear direction as a process that can be examined experimentally.

Natural fault systems are not necessarily characterized by deformation in a single persistent direction. Coseismic displacement is followed by postseismic and interseismic deformation, and the direction and magnitude of surface deformation may change during the earthquake cycle. For example, the 1946 Showa Nankai earthquake produced substantial subsidence of the Kochi Plain and uplift around Cape Muroto, while subsequent interseismic deformation has included uplift along parts of southwestern Japan (Baranes et al., 2018). Similarly, the 2011 Tohoku-Oki earthquake was followed by postseismic deformation that included uplift in areas that had undergone coseismic subsidence; this response reflects a combination of afterslip and viscoelastic relaxation rather than a simple elastic rebound (Freed et al., 2017). These observations emphasize that deformation recorded in geological materials may reflect multiple episodes with different displacement directions.

Despite the importance of deformation reversal, its influence on the microfabric of fine-grained shear-zone materials remains poorly constrained. A fabric generated during one episode of shear may survive partly into subsequent deformation, but the extent to which it is erased, rotated, or overprinted during reversal is not well understood. This problem is particularly relevant to clay-rich materials, in which particle-scale reorganization may influence bulk mechanical behavior and in which the final fabric may preserve information about previous deformation events (Dasent et al., 2025).

Fault-zone structures can preserve evidence of more than one deformation episode. Composite planar fabrics, for example, may contain shear planes with different orientations and shear senses, allowing successive stages of fault movement to be reconstructed when combined with stress inversion analysis (Sakai et al., 2024). Such observations indicate that the fabric of a fault zone may represent a superposition of deformation events rather than a single episode of shear. At a smaller scale, microscopic characteristics of fault gouge have also been used as auxiliary evidence for identifying active or potentially active faults. Li et al. (2022), for example, documented discontinuous microcracks and S-C fabrics in fault gouge from the Longmenshan Fault Zone and showed that systematic differences in gouge microstructure and mineralogical composition can be useful for distinguishing fault zones with different levels of activity. These studies demonstrate the potential of structural and microstructural fabrics to retain information on fault activity and deformation history.

However, these studies primarily document naturally developed fault-zone fabrics and their relationship to fault activity or stress history. How a reversal in shear direction is itself recorded in clay-rich material remains poorly constrained. In particular, it is not clear whether a fabric generated during one episode of shear is erased by subsequent deformation in the opposite direction or whether part of the earlier fabric is retained and reorganized. This question provides the basis for the present experimental study.

The central objective of this study is to determine how repeated reversal of shear is recorded in clay-rich microfabric and what elements of an earlier fabric survive subsequent deformation in the opposite sense. The Jin'nosuke-dani landslide provides the experimental material and a natural structural reference because its basal slip zone and magnetic fabric have been previously characterized (Kawamura et al., 2007, 2008). The experiment is not intended to reproduce the natural landslide history; rather, it isolates the effect of alternating shear direction under controlled normal stress.

The study combines repeated reversal direct-shear experiments with SEM, SP-μCT, and AMS. SEM provides high-resolution observations of clay-particle organization and localized deformation, SP-μCT provides three-dimensional information on the experimental fabric, and AMS provides a bulk-scale constraint on magnetic fabric that complements the limited fields of view of SEM and SP-μCT. Particular attention is given to the transverse Kmax orientation and its relationship to particle and clast rotation.

We test the working hypothesis that reversal of shear does not completely erase the fabric generated during the preceding deformation episode. Instead, part of the earlier fabric is expected to be retained, rotated, disrupted, and overprinted, producing a composite fabric. If such a response is characteristic of repeated reversal, it may help constrain the interpretation of natural clay-rich shear zones, although it should not be used as a standalone diagnostic of tectonic origin.

2 Geological setting and natural shear fabric

2.1 Geological and geomorphological setting

The Jin'nosuke-dani landslide is located in the Hakusan region of central Japan (Fig. 1), within a mountainous area characterized by steep slopes and deeply incised valleys. The landslide is developed within sedimentary rocks consisting mainly of shale and sandstone. The regional geology and stratigraphic relationships of the study area have been described previously by Kano et al. (1999) and Yamazaki (1988).

The landslide mass extends along the Jin'nosuke-dani and associated valley systems and is characterized by a complex internal structure consisting of multiple landslide blocks and shear zones (Figs. 1 and 2). The landslide is bounded by steep valley slopes, and the distribution of the landslide mass is closely related to the local topography and geological structure.

Previous investigations identified clay-rich basal slip zones within the landslide mass and documented structural fabrics associated with downslope movement (Isobe, 1996; Kawamura et al., 2007, 2008). These studies demonstrated that the basal slip zone contains strongly sheared shale and clay-rich materials and that the shear structures have a consistent relationship with the downslope movement direction.

The Jin'nosuke-dani landslide is characterized by seasonal displacement, with movement becoming particularly pronounced during periods of increased water availability. The present-day displacement rate has been reported to reach approximately 5 cm yr^{-1} during active periods (Kawamura et al., 2008). This continuing movement provides an opportunity to examine the microstructures preserved within an actively deforming landslide slip zone.

2.2 Basal slip zone and structural characteristics

The basal slip zone consists mainly of strongly sheared shale and clay-rich material. In the field, the sheared shale contains fragmented and locally rotated rock clasts embedded in a fine-grained clay-rich matrix (Fig. 2). Shear structures including Riedel-type structures are developed within the slip zone, and their orientations indicate a predominantly downslope sense of shear.

The basal slip zone also contains white to pale-colored clay-rich material. The clay-rich zone is spatially associated with the sheared shale and represents the principal fine-grained material examined in the present study. The structural relationship between the clay-rich material and the surrounding sheared shale provides an important field constraint for interpreting the fabrics produced during the laboratory experiments.

Previous structural and magnetic-fabric studies of the Jin'nosuke-dani landslide demonstrated that the preferred orientations of the basal slip-zone materials are consistent with the inferred direction of landslide movement (Kawamura et al., 2007, 2008). These independent field constraints are particularly important for the present study because they allow the experimentally and microscopically observed fabrics to be compared with a known deformation direction.

The combination of an actively moving landslide, well-developed basal shear zones, and previously established structural and magnetic fabrics makes the Jin'nosuke-dani landslide a suitable natural laboratory for investigating the development and preservation of clay-rich shear fabrics.

3. Materials and methods

3.1 Sampling and sample characterization

Samples were collected from the basal slip zone of the Jin'nosuke-dani landslide. The materials examined in this study consist mainly of sheared black shale and white clay-rich material exposed within the active slip zone (Fig. 2). The samples were collected in a water-containing state and were maintained in this condition prior to laboratory testing to minimize changes in their natural physical state.

The particle-size distribution and clay-mineral composition of the samples were determined prior to the shear experiments (Fig. 3). The clay fraction consists mainly of illite, kaolinite, and chlorite, with a minor contribution from smectite. These mineralogical characteristics are consistent with the fine-grained nature of the basal slip-zone material and provide the mineralogical context for interpreting the SEM and AMS results.

Two initial sample conditions were prepared for the direct shear experiments. The first consisted of undisturbed samples that retained the natural structure of the slip-zone material. The second consisted of slurry samples prepared by passing the water-containing material through a 250 μm sieve.

3.2 Direct shear experiments

Direct shear experiments were conducted using a single-plane direct shear apparatus manufactured by Seiken-sha Co., Ltd. The specimens were cylindrical discs with a diameter of 50 mm and a height of 30 mm. All specimens were tested in their water-containing state to minimize changes in the physical condition of the natural slip-zone material.

Three levels of normal stress, 0.4, 0.8, and 1.6 MPa, were applied in the experiments. These values were selected to represent the range of normal stresses expected from variations in overburden pressure within the landslide body. The maximum applied normal stress of 1.6 MPa approximately corresponds to the estimated maximum overburden pressure at the basal slip zone, whereas 0.4 and 0.8 MPa represent lower loading conditions associated with shallower portions of the landslide mass.

Before shear deformation, all specimens were subjected to a pre-consolidation period of 1000 min under the prescribed normal stress. The specimens were then subjected to ten repeated shear cycles, with the shear direction reversed after each cycle. Thus, the experimental procedure involved alternating shear in opposite directions rather than monotonic displacement in a single direction. Shear stress and vertical displacement were continuously recorded automatically by the testing apparatus. The experiments were terminated after completion of the predetermined ten shear cycles. The repeated cycles were used to characterize the frictional response of the materials and to obtain specimens representing a reproducible cumulative state of shear deformation for subsequent microstructural observations.

The resulting shear-stress and displacement records were used to characterize the mechanical response of the undisturbed and slurry materials under different normal-stress conditions (Figs. 4 and 5).

The experimental design was therefore used for two complementary purposes: characterization of the frictional response under representative gravitational loading and examination of the cumulative microstructural modification produced by the prescribed reversal-shear procedure. The ten-cycle endpoint should not be interpreted as a natural equivalent of the number of movements experienced by the landslide.

3.3 Microstructural observations

Microstructural observations were conducted on the experimentally deformed samples to characterize the fabric produced by repeated reversal shear. The natural microfabric of the Jin'nosuke-dani basal slip zone has been described in detail by Kawamura et al. (2007); it is used here as a previously established natural reference rather than re-described in detail.

3.3.1 SEM observations

After completion of the shear experiments, portions of the experimentally deformed samples were carefully collected for SEM observation. The samples were prepared by freeze-drying and resin embedding to minimize disturbance of the microfabric during drying. Pore water was replaced using ethyl alcohol and tri-butyl alcohol, and the samples were embedded in Quetol 651 resin (Nisshin EM Co., Ltd.) following the procedure of Takizawa et al. (1995).

The resin-embedded samples were sectioned and polished for SEM observation. The samples were coated with Au–Pd for secondary-electron imaging and with carbon for backscattered-electron imaging. SEM observations were performed at an accelerating voltage of 15 kV and a beam current of approximately 80 μA.

The observations focused on the development of clay-particle orientations, localized shear structures, fragmentation and rotation of shale clasts, and other microstructural features produced by repeated shear.

3.3.2 Synchrotron radiation micro-X-ray computed tomography

Three-dimensional microfabric of the experimentally deformed samples was examined using synchrotron radiation micro-X-ray computed tomography (SP-μCT). Measurements were conducted at beamline BL47XU of the SPring-8 synchrotron radiation facility, Hyogo, Japan.

Specimens approximately 0.5 × 0.5 × 2 mm in size were prepared from the resin-embedded experimental samples. An X-ray beam energy of 25 keV was used to obtain transmitted images with sufficient contrast for characterization of the internal microstructure.

The SP-μCT observations were used to examine the three-dimensional arrangement of the experimentally produced microfabric and to complement the two-dimensional SEM observations.

3.4 Anisotropy of magnetic susceptibility

AMS measurements were conducted on the natural slip-zone materials and experimentally sheared specimens to characterize the preferred orientation of magnetic susceptibility carriers associated with the shear fabric. For the experimentally sheared samples, subsamples were cut from the deformed specimens after completion of the ten-cycle experiments. AMS was used as a complementary bulk-scale indicator because it integrates the magnetic susceptibility fabric over a larger volume than the SEM and SP-μCT observations.

Magnetic susceptibility was measured in three orthogonal directions, and the principal susceptibility axes (Kmax, Kint, and Kmin) were calculated for each specimen. The degree and shape of magnetic anisotropy were evaluated using the anisotropy parameters P′ and T.

High-field and low-field magnetic susceptibilities were also measured to evaluate the relative contribution of paramagnetic and ferromagnetic constituents. The Khf/Klf ratio was calculated for each sample. Because the slip-zone materials contain abundant phyllosilicate minerals, including illite, kaolinite, and chlorite, the observed magnetic fabric is interpreted primarily in relation to the phyllosilicate-rich matrix, while recognizing that the AMS signal may include contributions from other magnetic constituents. AMS is not treated as a direct measurement of individual clay-particle long axes.

For the experimentally deformed specimens, the orientations of Kmax and Kmin were compared with the imposed shear direction. For the natural material, the magnetic fabric was compared with the independently established downslope movement direction reported by Kawamura et al. (2007, 2008). These comparisons were used to evaluate the relationship among local microfabric, bulk magnetic fabric, and deformation direction.

4. Results

4.1 Mechanical behavior during shear experiments

The repeated shear tests show changes in shear resistance during successive cycles. Because the shear direction was reversed after each cycle, the sign of the recorded shear stress changed with the imposed direction (Fig. 4). Negative values therefore indicate the direction of shear relative to the reference coordinate system and do not represent negative shear strength; the magnitude of shear stress represents the shear resistance of the material. Under all three normal-stress conditions, both undisturbed and slurry samples underwent repeated deformation accompanied by changes in shear stress and vertical displacement. The magnitude and evolution of shear stress differed between the two sample types, indicating that the initial physical state of the slip-zone material influenced its mechanical response.

The experiments conducted at 1.6 MPa are particularly relevant to the natural slip zone because this normal stress approximately corresponds to the maximum estimated overburden pressure. The 0.4 and 0.8 MPa experiments provide lower-stress conditions representing spatial variations in gravitational loading associated with differences in overburden thickness within the landslide body.

The relationship between applied normal stress and shear resistance shows an overall increase in shear resistance with increasing normal stress (Fig. 5). The undisturbed and slurry samples show different mechanical responses, indicating that disruption of the original material state influences the measured shear resistance.

The experimental products also show localized deformation structures after ten repeated shear cycles. These structures are more clearly developed in the samples subjected to the higher normal stress. The deformed samples were subsequently used for SEM, SP-μCT, and AMS analyses to examine the microstructural and magnetic fabrics associated with the cumulative shear deformation.

4.2 Magnetic fabrics of sediments and rocks in the slip zone

The Khf and Klf values of the sheared black shale were 8.95×10^{-4} and 10.58×10^{-4} $m^3 kg^{-1}$, respectively, whereas those of the white clay were 13.06×10^{-4} and 17.03×10^{-4} $m^3 kg^{-1}$, respectively (Table S2). The Khf/Klf ratios exceed 0.7 for both materials, indicating that paramagnetic minerals make a substantial contribution to the low-field magnetic susceptibility. Given the mineralogical composition of the slip-zone materials, phyllosilicates such as illite, kaolinite, and chlorite are likely to contribute substantially to the observed magnetic fabric.

The principal AMS directions of the natural and experimentally sheared black shale and white clay are shown in Fig. 6. In the natural slip-zone material, Kmax is approximately parallel to the downslope movement direction, consistent with the previously documented natural magnetic fabric (Kawamura et al., 2007, 2008). In the experimentally sheared samples, Kmax is approximately horizontal and oriented perpendicular to the imposed shear direction, whereas Kmin is generally subvertical. This transverse Kmax orientation is distinct from a simple fabric aligned with the final shear direction and is a key observation for interpreting the cumulative effect of reversal shear.

4.3 Microfabric produced by repeated shear

SEM and SP-μCT observations reveal microstructural changes associated with repeated reversal shear in the experimentally deformed samples (Fig. 7). SEM observations show preferentially oriented clay flakes, fragmented and locally rotated shale clasts, and sigmoidal or asymmetric structures. The corresponding SP-μCT images show the three-dimensional organization of the experimentally deformed material. In the white-clay samples, SEM observations show a pronounced preferred orientation of clay flakes and locally abundant face-to-face contacts, while SP-μCT shows their three-dimensional arrangement. Together, these observations indicate that an organized clay-rich fabric persists after completion of the ten-cycle test.

The principal AMS directions of the experimentally deformed materials are shown in Fig. 6. In both the sheared black shale and white clay, Kmax is approximately horizontal and oriented perpendicular to the imposed shear direction, whereas Kmin is generally subvertical. This transverse Kmax orientation indicates that the bulk magnetic fabric is not simply aligned with the direction of the final shear cycle.

SEM observations show preferentially oriented clay flakes in the sheared material (Fig. 7A, B). Fragmented and locally rotated shale clasts are also present, together with sigmoidal and asymmetric structures. These features indicate localized deformation of the clay-rich material during repeated shear.

The corresponding SP-μCT images provide three-dimensional views of the internal arrangement of the experimentally deformed material (Fig. 7C, D). The three-dimensional observations complement the two-dimensional SEM observations and show the internal organization of the clay-rich material after repeated shear.

In the white-clay samples, SEM observations show a pronounced preferred orientation of clay flakes and locally abundant face-to-face contacts (Fig. 7E, F). The corresponding SP-μCT images show the three-dimensional arrangement of the experimentally sheared white clay (Fig. 7G, H). These observations indicate that repeated reversal shear produces an organized clay-rich fabric that persists in the specimens after completion of the ten-cycle test.

The experimental microfabric is compared with the natural basal slip-zone fabric previously documented by Kawamura et al. (2007) in the Discussion.

5. Discussion

5.1 Experimental fabric and the natural slip-zone reference

The experimentally deformed samples show clay-rich fabrics and localized deformation structures that are broadly comparable to those documented previously in the natural basal slip zone of the Jin'nosuke-dani landslide

(Kawamura et al., 2007). The natural study reported preferred clay-particle orientations and shear-related structures within strongly sheared shale and clay-rich material. These observations provide useful context for the present experiments, but the natural fabric is not re-described here because its microstructural characteristics have already been documented in detail.

The important result of the present experiments is not simply that shear can produce a clay fabric, which is well established, but that repeated reversal produces a final fabric that reflects cumulative deformation rather than a single shear direction. SEM and SP-μCT show preferred orientations, localized deformation, and rotated clasts after ten alternating cycles. The natural and experimental fabrics may therefore share some morphological features, but their deformation histories need not be the same.

The Jin'nosuke-dani material is especially useful for this experiment because the natural slip zone has an independently established downslope kinematic framework. Nevertheless, the natural fabric may contain inherited structures from the host shale as well as structures produced during gravitational sliding. The laboratory experiment therefore provides a controlled process reference rather than a direct reconstruction of the natural deformation history.

5.2 Multi-scale characterization of reversal-related fabric

The combination of SEM, SP-μCT, and AMS provides complementary constraints at different spatial scales. SEM resolves clay-particle contacts, preferred orientations, localized structures, and rotated clasts at high spatial resolution. SP-μCT extends the observations into three dimensions and shows whether organized structures persist through the imaged volume. AMS integrates magnetic susceptibility over a substantially larger specimen volume and therefore provides an independent constraint on whether an orientation tendency identified locally has a coherent bulk-scale expression.

The three methods should not be regarded as interchangeable. SEM and SP-μCT provide morphological observations of the experimentally deformed material, whereas AMS is an indirect proxy for the preferred orientation of magnetic susceptibility carriers. The Khf/Klf ratios indicate a substantial paramagnetic contribution, and the abundance of phyllosilicates supports a significant contribution from the clay-rich matrix. Nevertheless, other magnetic constituents may contribute to the AMS signal. The significance of the transverse Kmax orientation therefore lies in its agreement with the local microstructural observations rather than in treating Kmax as a direct measurement of individual clay-particle long axes.

The natural fabric documented by Kawamura et al. (2007) provides a useful reference for recognizing structures that can occur in the Jin'nosuke-dani slip zone, but the present study does not assume that those natural structures were produced by the same reversal history imposed in the laboratory. This distinction is important when the experimental results are later considered as a possible criterion for differentiating tectonic and landslide shear zones.

The natural basal slip-zone fabric documented by Kawamura et al. (2007) includes preferred clay-particle orientations, fragmented and rotated shale fragments, asymmetric shear-related structures, and a preferred magnetic fabric associated with the field-defined shear direction. The experimental observations demonstrate that repeated reversal shear can produce microstructural reorganization of clay-rich material that is broadly comparable to these natural features.

The direct-shear experiments were originally conducted to characterize the frictional response of the slip-zone materials under normal stresses representative of gravitational loading. The ten-cycle reversal-shear endpoint also provides a reproducible state for examining the cumulative effects of repeated deformation. Although the laboratory experiments cannot reproduce the timescale or displacement rate of the natural landslide, the correspondence between the experimental and natural fabrics provides a process-based constraint on the interpretation of the natural slip zone.

The present-day displacement rate of the Jin'nosuke-dani landslide is approximately 5 cm yr^{-1} during the active season, which is several orders of magnitude lower than the shear displacement rate imposed in the laboratory experiments. Consequently, the natural fabric should not be regarded as a direct equivalent of the experimental fabric. Rather, the natural fabric is interpreted as the cumulative product of inherited geological fabric and subsequent gravitational deformation, whereas the laboratory experiments identify processes by which repeated shear may modify clay-rich material.

Importantly, the correspondence between the natural and experimental fabrics does not by itself exclude an inherited component of the natural fabric. The agreement among clay orientation, AMS, field shear structures, and downslope movement direction provides evidence that the natural fabric was substantially modified by gravitational shear, rather than proving that all of the observed fabric formed during landsliding.

5.3 Gouge rotation and bulk fabric development during reversal shear

The combined SEM, SP-μCT, and AMS observations are consistent with a rotational mode of deformation during repeated reversal shear. SEM observations reveal localized particle reorganization and rotation of shale-derived clasts, whereas SP-μCT demonstrates a three-dimensional organization of the experimentally deformed material. These observations suggest that deformation was not accommodated solely by translation along a single shear direction, but also involved rotation and reorganization of gouge-like material.

The transverse Kmax orientation provides a bulk-scale constraint for this interpretation. In both experimentally deformed materials, Kmax is approximately horizontal and oriented perpendicular to the imposed shear direction. We interpret this geometry as consistent with rotation and rolling of elongated particles, particle aggregates, or fragmented shale clasts within the gouge-like material. During reversal, the sense of relative motion changes and the structures generated during the preceding shear cycle are subjected to deformation in the opposite direction. The resulting fabric is therefore not expected to retain a simple relationship with the final shear direction.

This interpretation is consistent with the broader observation that fault-zone fabrics can preserve evidence of multiple deformation stages. Sakai et al. (2024) demonstrated that composite planar fabrics in the Shionohira and Kuruma faults can be used, together with stress inversion analysis, to reconstruct multiple stages of fault movement and stress history. Their results emphasize that structures within a fault zone may represent a superposition of deformation episodes rather than a single kinematic event. Our experimental results provide a complementary perspective at the microstructural scale: rather than identifying separate shear planes associated with different natural events, we show that reversal of shear can produce a composite fabric within the same clay-rich material.

The proposed rolling mechanism should be regarded as an interpretation rather than a direct observation of particle trajectories. AMS alone cannot demonstrate rolling, and Kmax is not a direct measurement of the long axis of individual clay particles. Its value here is that the bulk-scale transverse magnetic fabric is consistent with the localized rotation and reorganization observed by SEM and SP-μCT. The agreement among the three methods provides a stronger basis for interpreting the final fabric than any one method alone.

Microstructural characteristics have previously been used as auxiliary criteria for identifying active fault zones. Li et al. (2022), for example, showed that fault gouges from minor-surface-rupture faults in the Longmenshan Fault Zone possess systematic microscopic and mineralogical characteristics that differ from those of more intensely active faults. Their study demonstrates that fault activity can leave recognizable signatures at the microscopic scale. The present study extends this concept from the identification of fault activity to the identification of deformation history. Rather than focusing on the presence or absence of a particular microstructural feature, we focus on the organization of fabric produced when the direction of shear is repeatedly reversed.

If reversal-related fabric memory is preserved in natural fault gouges, it may provide an additional criterion for distinguishing tectonic shear zones from gravitational landslide slip zones. A landslide slip zone may develop strong shear fabrics during downslope movement, but its fabric would not necessarily be expected to contain the same rotational overprint produced by repeated reversals of shear direction. This distinction remains a hypothesis at present and requires testing using natural fault gouges and landslide slip-zone materials with independently constrained deformation histories.

5.4 Fabric memory during reversal deformation and its potential diagnostic value

Fault-zone fabrics commonly record more than one stage of deformation. Composite planar structures can preserve different shear senses and orientations, allowing successive stages of fault movement and stress history to be reconstructed (Sakai et al., 2024). At the microscopic scale, differences in fault-gouge microstructure have also been used as auxiliary evidence for identifying active fault zones (Li et al., 2022). These studies demonstrate that deformation history may be preserved in fault-zone fabrics across multiple spatial scales. The question addressed here is more specific: how does a reversal in shear direction modify an existing clay-rich fabric, and what part of the preceding fabric survives the reversal?

Reversal or modification of deformation is an important feature of natural tectonic systems. During an earthquake cycle, coseismic displacement is followed by postseismic and interseismic deformation, and the direction and magnitude of deformation may change with time. Postseismic deformation may involve afterslip and viscoelastic relaxation rather than a simple elastic rebound (Freed et al., 2017). The significance of this cycle for the present study is conceptual: a fault-zone fabric may integrate several deformation episodes whose individual contributions are difficult to separate after the fact.

The Nankai subduction zone provides an example of changing deformation through the earthquake cycle. Geological and geodetic observations indicate coseismic deformation followed by longer-term interseismic strain accumulation (Baranes et al., 2018). Such observations illustrate why a tectonic shear-zone fabric need not represent a single, uniform deformation stage.

These observations raise a question that is rarely addressed from a microstructural perspective: how is a reversal in deformation direction recorded in the fabric of fine-grained shear-zone materials? A shear fabric generated during one deformation episode may be modified when the direction of deformation subsequently reverses. Whether the preceding fabric is completely erased, simply overprinted, or partly preserved while being reorganized remains poorly constrained. Natural fault-zone materials are difficult to use for resolving this problem because their complete deformation histories are rarely known.

The present experiments provide a controlled approach to this question. Because the shear direction was deliberately reversed after each cycle, the final microfabric represents the cumulative response to alternating deformation rather than the product of a single shear direction. The experimentally generated fabric can therefore be regarded as a record of deformation history, or experimental fabric memory.

The observations suggest that reversal shear does not simply erase the fabric produced during the preceding shear cycle. Instead, elements of the pre-existing fabric are retained while being rotated, fragmented, and reorganized during subsequent deformation. The transverse Kmax orientation observed by AMS is consistent with this interpretation because it indicates a preferred bulk-scale orientation that is not parallel to the final shear direction.

We therefore propose that repeated reversal produces a rotational fabric memory. During one shear direction, asymmetric structures develop within the gouge-like material. When the shear direction reverses, these structures are subjected to deformation in the opposite sense. Rather than being completely destroyed, some components rotate and roll, changing their orientation while retaining part of the structural information generated during the preceding cycle. Repeated reversal consequently produces a composite fabric containing remnants of multiple deformation directions.

The structural significance of this result is that a fine-grained shear zone may retain evidence of more than one deformation episode even when the final fabric is not obviously bimodal. In a tectonic setting, such composite fabrics may arise from successive deformation episodes with changing kinematics. A reversal-related fabric should therefore be considered as a possible record of deformation history rather than as a simple indicator of the final shear direction. Whether the same process can distinguish tectonic fault gouges from gravitational landslide slip zones remains an open question that requires comparison with natural materials of independently constrained kinematic histories.

A limitation of the present experiment is that SEM, SP-μCT, and AMS measurements were performed after completion of the ten-cycle experiment. The data therefore do not resolve the progressive development, rotation, or partial erasure of the fabric during individual cycles. The observed fabric is the integrated product of the imposed deformation sequence. Experiments terminated after individual cycles, or in-situ measurements of fabric evolution, are needed to test the proposed rotational-memory mechanism directly.

Nevertheless, the present results establish an experimentally testable framework: repeated reversal can produce a composite clay-rich fabric whose geometry differs from that of a simple unidirectional shear fabric. The combination of freeze-drying and resin embedding for SEM, three-dimensional SP-μCT imaging, and bulk AMS provides complementary observations across spatial scales. This approach can be applied in future studies to natural fault gouges and landslide slip zones to determine whether reversal-related fabric memory can be recognized independently of field-scale kinematic evidence.

6. Conclusions

The experiments demonstrate that repeated reversal shear can produce a cumulative clay-rich fabric that differs from a simple unidirectional shear fabric. The principal results are as follows.

(1) Direct-shear experiments at 0.4, 0.8, and 1.6 MPa produced systematic changes in shear resistance during ten reversal cycles.

(2) SEM and SP-μCT reveal preferred clay-flake orientations, localized deformation, fragmented and rotated shale clasts, and a three-dimensional organized fabric after reversal shear.

(3) AMS provides a bulk-scale constraint on the experimental fabric; Kmax is approximately horizontal and perpendicular to the imposed shear direction. This geometry is consistent with rotational reorganization of gouge-like material when considered together with SEM and SP-μCT.

(4) Reversal shear does not simply erase the fabric produced during the

preceding cycle. Elements of the earlier fabric can be retained while being rotated, disrupted, and overprinted, producing experimental fabric memory.

(5) The results support a process-based interpretation in which the final fabric records cumulative deformation history rather than only the last shear direction. Application to natural tectonic faults and landslide slip zones remains a testable hypothesis.

(6) Because observations were made only after ten cycles, cycle-by-cycle fabric evolution remains unresolved and should be addressed in future experiments.

7. Acknowledgements

The authors gratefully acknowledge Dr. Toshitsugu Yamazaki (National Institute for Advanced Industrial Science and Technology, Japan) for help in undertaking AMS and VSM measurements. Mr. Tetsuro Kitahara provided support for the investigation of the Jin'nosuke-dani landslide, while the experiments on clay samples were conducted with the assistance of Mr. Takashi Yoshida from the Core Lab of Oyo Corporation. This study was partly supported by a Grant-in-Aid from the SABO Technical Center.

Funding and competing interests

Funding: This study was partly supported by a Grant-in-Aid from the SABO Technical Center.

Competing interests: The author declares that he has no financial or non-financial competing interests.

Declaration of Generative AI and AI-assisted technologies in the writing process

During the preparation of this manuscript, the author used ChatGPT (OpenAI) for language editing and for checking the organization and clarity of the English text. The author reviewed and revised all AI-assisted output and takes full responsibility for the content.

References

Dasent, J., Wright, V., Scharer, K.M., Manga, M. & Kilburn, R. (2025). Memory and jamming in fault zone sediments. Communications Earth & Environment, 6, 998.

https://doi.org/10.1038/s43247-025-02952-4

Freed AM, Hashima A, Becker TW, Okaya DA, Sato H, Hatanaka Y (2017) Resolving depth-dependent subduction zone viscosity and afterslip from postseismic displacements following the 2011 Tohoku-oki, Japan earthquake. Earth and Planetary Science Letters 459:279–290. https://doi.org/10.1016/j.epsl.2016.11.040

Haines SH, Kaproth B, Marone C, Saffer D, van der Pluijm B (2013) Shear zones in clay-rich fault gouge: A laboratory study of fabric development and evolution. Journal of Structural Geology 51:206–225. https://doi.org/10.1016/j.jsg.2013.01.002

Haines SH, van der Pluijm BA (2009) Clay fabric intensity in natural and artificial fault gouges: Implications for brittle fault zone processes and sedimentary basin clay fabric evolution. Journal of Geophysical Research: Solid Earth 114:B05401. https://doi.org/10.1029/2008JB005866

Housen BA (1997) Magnetic anisotropy of Barbados prism sediments. In: Shipley TH, Ogawa Y, Blum P, Bahr JM (eds) Proceedings of the Ocean Drilling Program, Scientific Results, Vol 156. Ocean Drilling Program, College Station, TX, pp 97–105. https://doi.org/10.2973/odp.proc.sr.156.010.1997

Housen BA, Sato T (1995) Magnetic anisotropy fabrics from the Cascadia accretionary prism. In: Carson B, Westbrook GK, Musgrave RJ, Suess E (eds) Proceedings of the Ocean Drilling Program, Scientific Results, Vol 146 (Pt 1). Ocean Drilling Program, College Station, TX, pp 233–254. https://doi.org/10.2973/odp.proc.sr.146-1.217.1995

Isobe A (1996) Countermeasure for the Jin'nosuke-dani landslide. Kisoko 24(6):88–94 (in Japanese).

Kano K, Harayama S, Yamamoto H, Takeuchi M, Uto K, Komazawa M, Hiroshima T, Sudo S (1999) Geological map of Japan 1:200,000 Kanazawa. Geological Survey of Japan, Tsukuba, NJ-53-12.

Kawamura K, Ogawa Y, Oyagi N, Kitahara T, Anma R (2007) Structural and fabric analyses of basal slip zone of the Jin'nosuke-dani landslide, northern central Japan: its application to the slip mechanism of decollement. Landslides 4(4):371–380. https://doi.org/10.1007/s10346-007-0094-z

Kawamura K, Ogawa Y, Kitahara T, Endo R, Anma R, Oyagi N (2008) Active basal slip zones in the Jin'nosuke-dani landslide, Mount Hakusan, Central Japan. Island Arc 17(2):183–184. https://doi.org/10.1111/j.1440-1738.2008.00613.x

Li Y, Chen L, Ran Y, Chang Y (2022) Microscopic characteristics of fault gouge in minor-surface-rupture faults: A case study in the Longmenshan Fault Zone, Eastern Tibetan. Frontiers in Earth Science 10:840667. https://doi.org/10.3389/feart.2022.840667

Mandl G (2000) Faulting in brittle rocks: An introduction to the mechanics of tectonic faults. Springer, Berlin.

Moore DE, Summers R, Byerlee JD (1989) Sliding behavior and deformation textures of heated illite gouge. Journal of Structural Geology 11(3):329–342. https://doi.org/10.1016/0191-8141(89)90072-2

Ramsay JG, Huber MI (1983) The techniques of modern structural geology, Volume 1: strain analysis. Academic Press, London.

Rathore JS, Courrioux G, Choukroune P (1983) Study of ductile shear zones (Galicia, Spain) using texture goniometry and magnetic fabric methods. Tectonophysics 98(1–2):87–109. https://doi.org/10.1016/0040-1951(83)90212-3

Sakai T, Kametaka M, Aoki K, Shimada K, Takagi H (2024) Estimation of kinematic and stress history by composite planar fabric and stress inversion analysis: Application to the Shionohira and Kuruma faults. Journal of the Geological Society of Japan 130:89–109. https://doi.org/10.5575/geosoc.2024.0001

Suda Y, Murata Y, Kikuchi T, Hanaoka N (1991) Physical properties database of rocks (PROCK). Geological Survey of Japan Open-file Report 155, 231 p.

Takizawa S, Kawata T, Ohno Y (1995) A method of fixation and freeze-drying of soft sediments containing water. Journal of the Geological Society of Japan 101:941–944 (in Japanese).

Tarling DH, Hrouda F (1993) The magnetic anisotropy of rocks. Chapman and Hall, London.

Tchalenko JS (1968) The evolution of kink-bands and the development of compression textures in sheared clays. Tectonophysics 6(2):159–174. https://doi.org/10.1016/0040-1951(68)90017-6

Yamazaki M (1988) Hakusan volcanic chain. In: Yamashita N, Kaseno Y, Itoigawa J (eds) Regional geology of Japan, Part 5, Chubu II. Kyoritsu Shuppan, Tokyo, pp 190–191.

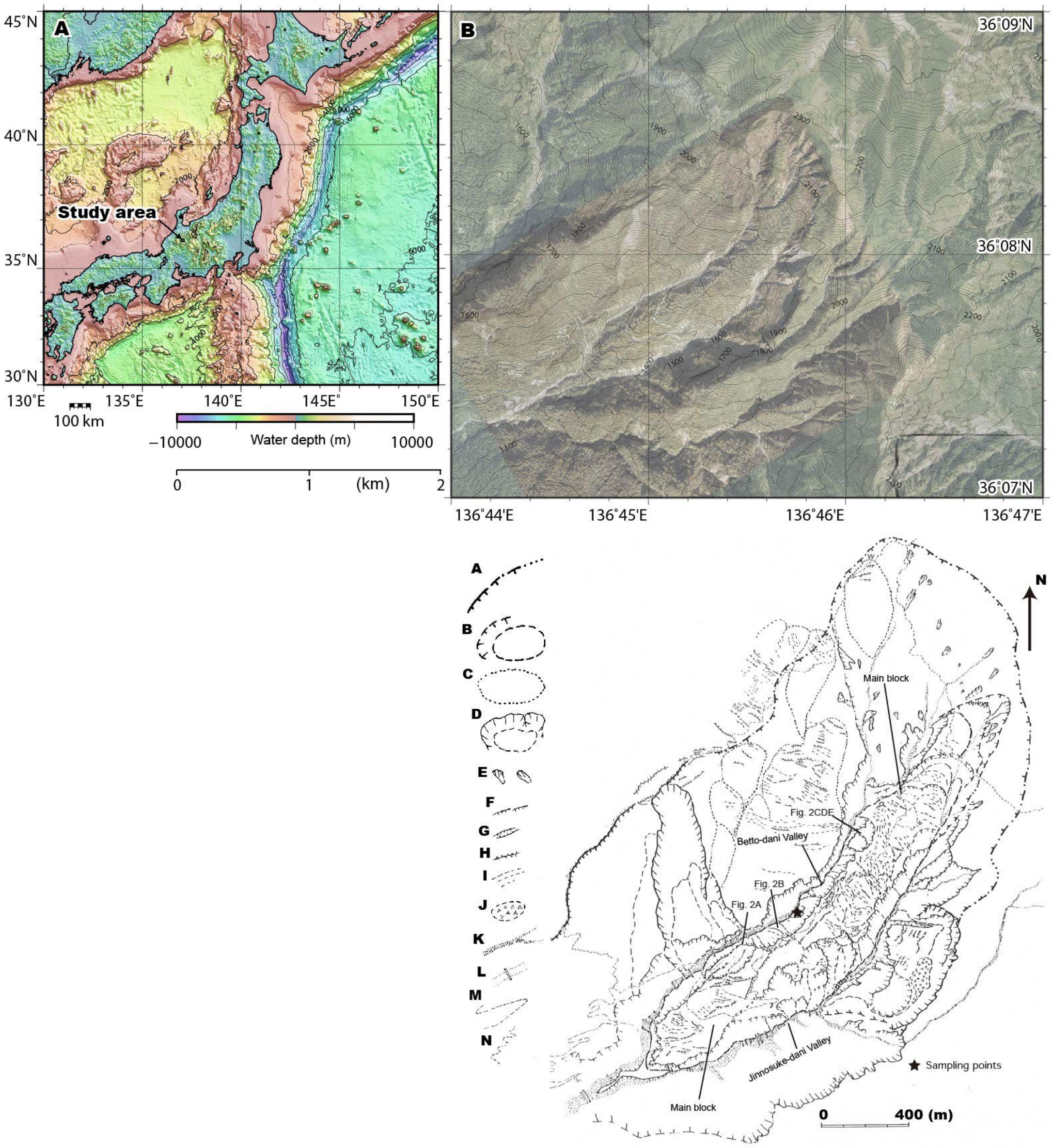

Figure 1. Location and geomorphological setting of the Jin'nosuke-dani landslide, Ishikawa Prefecture, central Japan. (A) Location of the study area in central Japan. (B) Topographic view of the Jin'nosuke-dani landslide and surrounding valleys. (C) Geological and geomorphological map showing the main landslide blocks, valleys, and sampling sites.

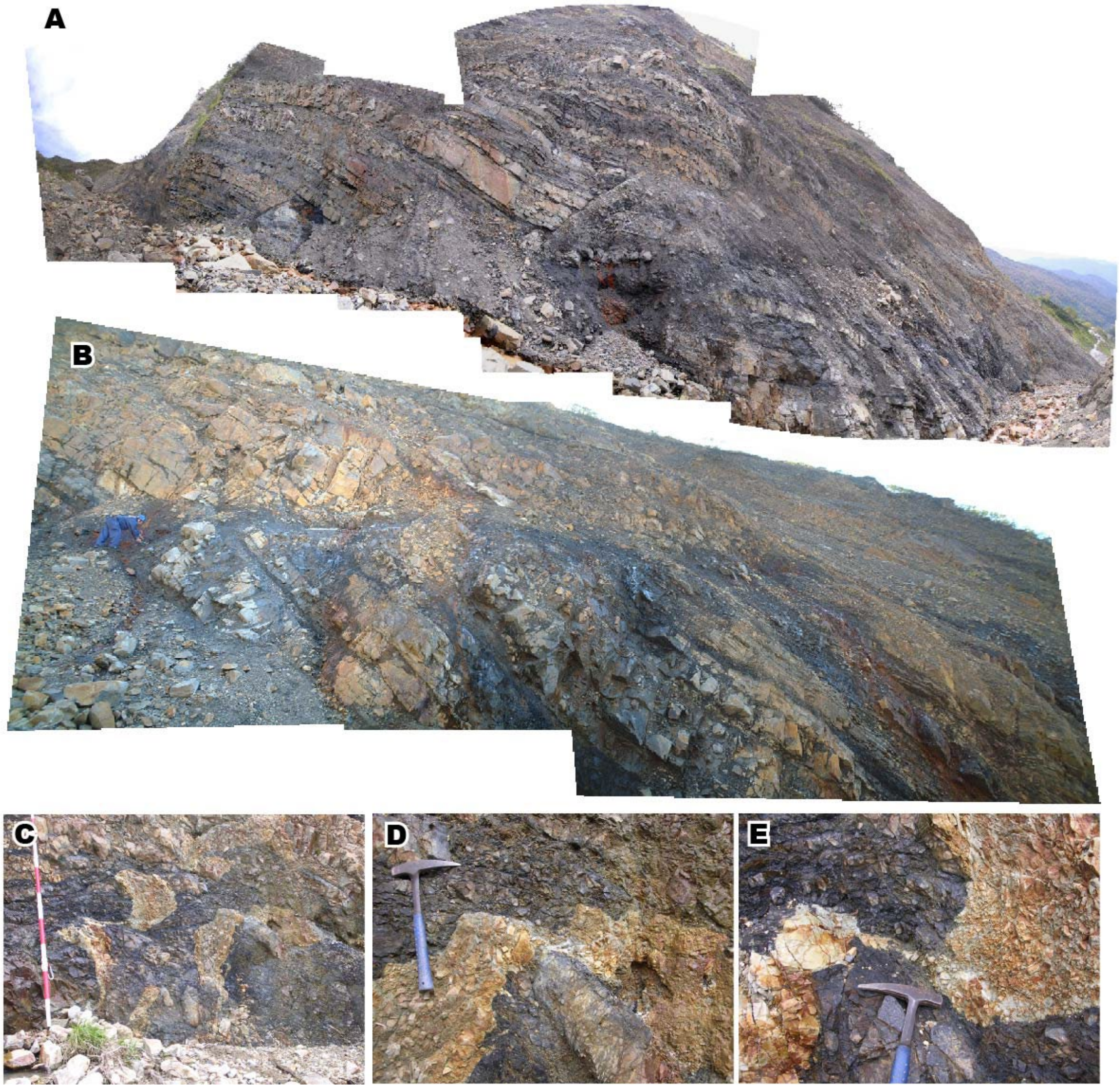

Figure 2. Geological and structural characteristics of the Jin'nosuke-dani landslide. (A) Large-scale view of the landslide mass. (B) Shale and sandstone beds exposed along the Betto-dani Valley. (C–E) Close-up views of sheared shale and clay-rich slip zones. The orientations of the principal shear structures are described in the text.

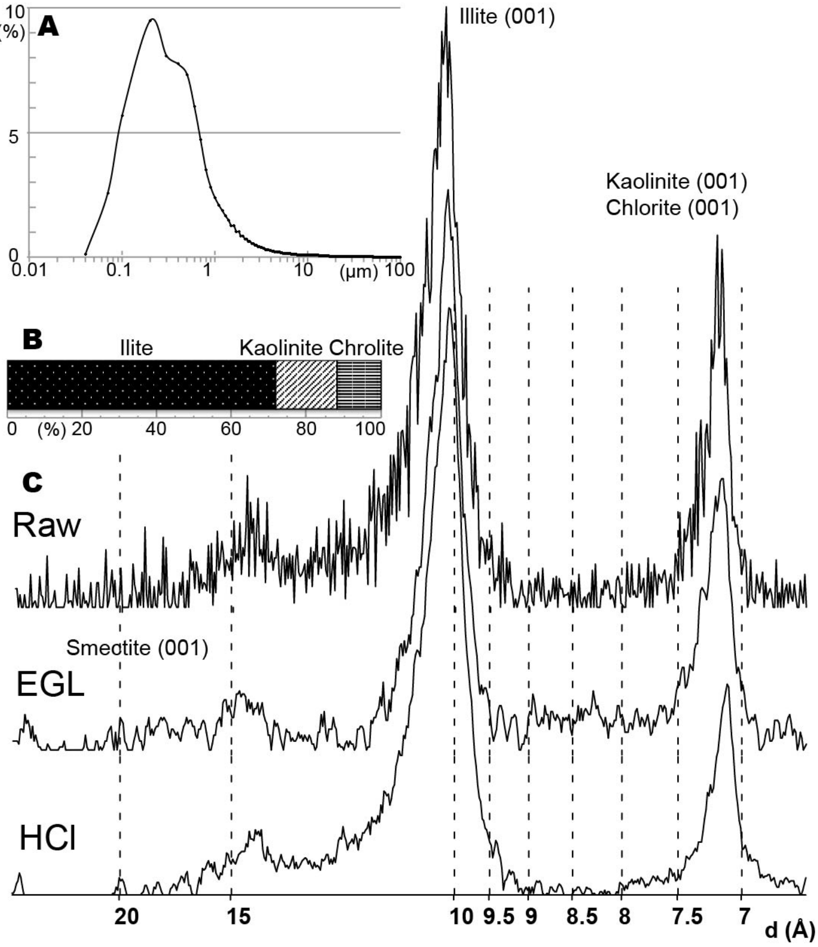

Figure 3. Particle-size characteristics and clay-mineral composition of the materials from the Jin'nosuke-dani slip zone. (A) Particle-size distribution. (B) Relative proportions of identified clay minerals. (C) X-ray diffraction patterns of the clay fraction under untreated (Raw), ethylene-glycolated (EG), and hydrochloric-acid-treated (HCl) conditions. The principal clay minerals are illite, kaolinite, and chlorite; smectite is detected in the glycolated sample.

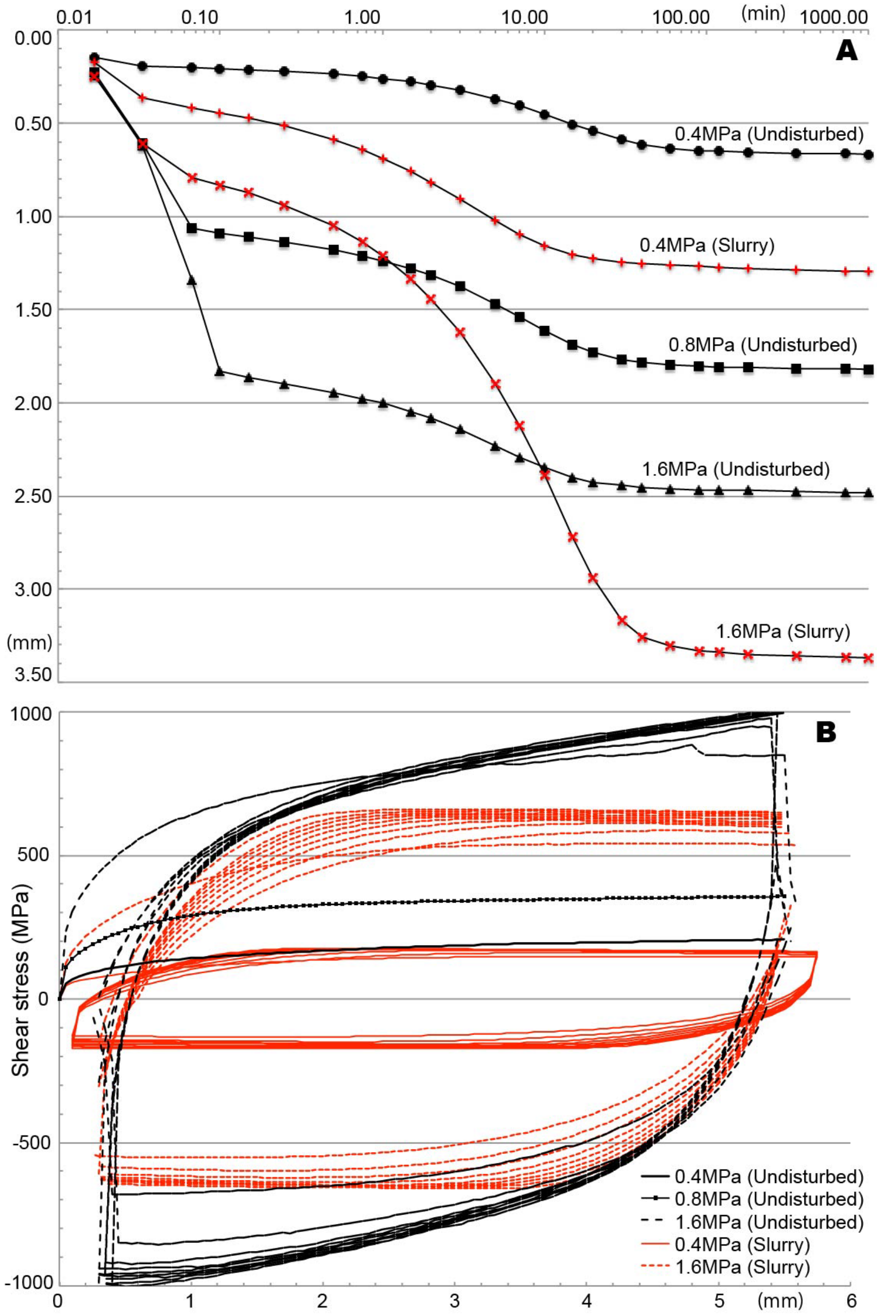

Figure 4. Mechanical response of the Jin'nosuke-dani slip-zone materials during repeated reversal direct shear. Results are shown for normal stresses of 0.4, 0.8, and 1.6 MPa. Shear stress and shear displacement are shown for undisturbed and slurry samples. The shear direction was reversed after each cycle. Because the sign of shear stress follows the imposed direction, negative values indicate reverse shear relative to the reference coordinate system and do not represent negative shear strength. The ten-cycle endpoint was used for

subsequent SEM, SP-μCT, and AMS observations.

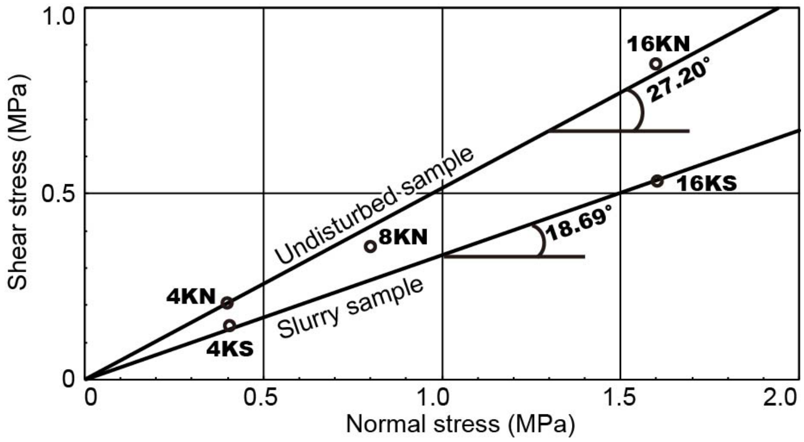

Figure 5. Relationship between applied normal stress and shear resistance obtained from the laboratory direct shear experiments. Results are shown for the undisturbed (4KN, 8KN, 16KN for 0.4, 0.8, and 1.6 MPa normal stress) and slurry samples (4KS and 16KS for 0.4 and 1.6 MPa normal stress). The applied normal-stress range of 0.4–1.6 MPa was selected to represent variations in gravitational loading associated with differences in overburden thickness within the landslide body.

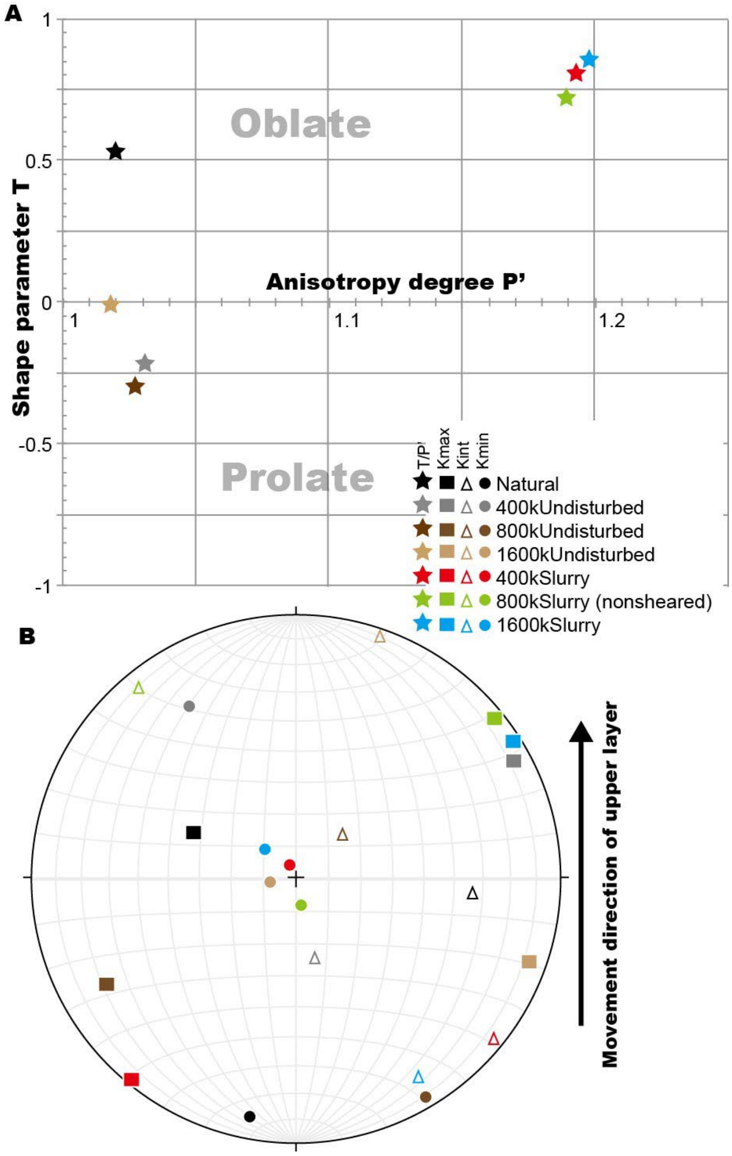

Figure 6. Magnetic fabrics of the natural and experimentally sheared slip-zone materials determined by anisotropy of magnetic susceptibility (AMS). (A) Plot of the anisotropy degree (P′) and shape parameter (T). (B) Equal-area stereographic projection of the principal susceptibility axes. Symbols distinguish natural and experimentally sheared samples and the applied normal-stress conditions. In the natural material, Kmax is approximately parallel to the downslope movement direction. In the experimentally deformed materials, Kmax is approximately horizontal and oriented perpendicular to the imposed shear direction, whereas Kmin is generally subvertical. The transverse Kmax orientation is interpreted as a bulk-scale constraint consistent with rotational reorganization of gouge-like material; it

is not treated as a direct image of individual particle long axes.

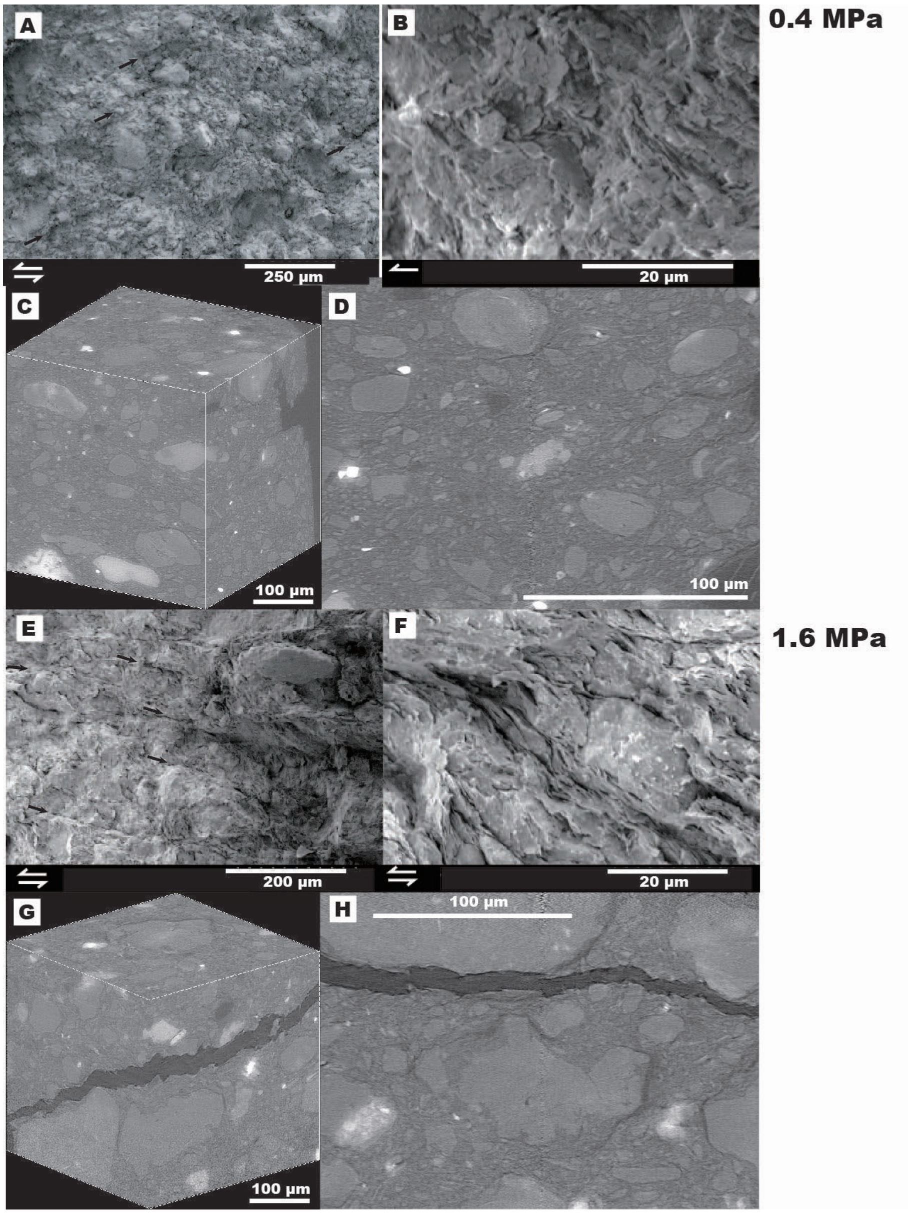

Figure 7. Microfabric of the experimentally deformed Jin'nosuke-dani slip-zone materials after ten repeated reversal-shear cycles. (A, B) SEM images of sheared black shale showing fragmented shale clasts, clay flakes, and localized shear-related structures. (C, D) SP-µCT images showing the three-dimensional arrangement of the experimentally deformed black shale and clay-rich material. (E, F) SEM images of experimentally sheared white clay showing preferred orientations of clay flakes and face-to-face contacts. (G, H) SP-µCT images showing the three-dimensional arrangement of the experimentally sheared white clay. Arrows indicate the imposed shear

direction during the final shear cycle and are provided only as a reference; they do not imply that the final fabric records only the last shear direction. Scale bars are shown in each panel.

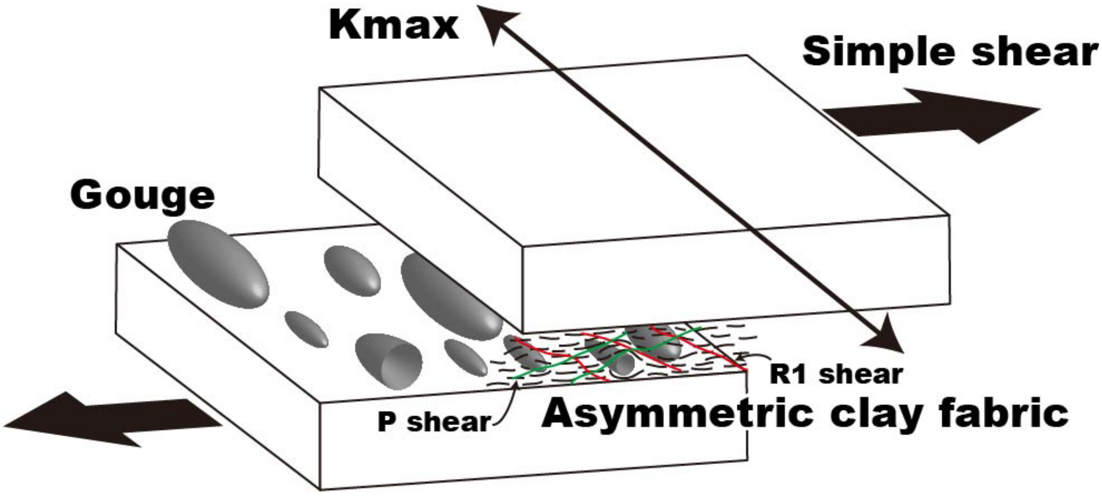

Figure 8. Conceptual model for fabric memory during repeated reversal shear. A fabric generated during one shear direction is partly retained during subsequent reversal, while particle and clast rotation, disruption, and reorganization produce a composite fabric. The final fabric therefore records cumulative deformation history rather than only the last shear direction.

Supplementary Tables

Table S1. Experimental conditions and principal mechanical results of the laboratory direct shear tests. Sample type, applied normal stress, pre-consolidation time, number of shear cycles, shear displacement, shear stress, and vertical displacement are summarized for each experiment.

Sample	Repeated times	Shear displacement (mm)	Shear stress (kPa)	Vertical displacement (mm)	Normal stress (kPa)	Cumulative displacement (mm)
0.4MPa Undisturbed	1	5.50	207.00	0.10	399.61	5.50
0.8MPa Undisturbed	1	5.50	356.64	0.18	800.00	5.50
1.6MPa Undisturbed	1	5.50	848.34	0.14	1599.15	5.50
1.6MPa Undisturbed	2	5.50	946.88	0.56	1599.05	16.49
1.6MPa Undisturbed	3	5.50	979.09	0.72	1599.05	27.49
1.6MPa Undisturbed	4	5.50	995.71	0.82	1598.48	38.49
1.6MPa Undisturbed	5	5.45	1005.30	0.89	1598.59	49.48
1.6MPa Undisturbed	6	5.45	1006.40	0.94	1599.15	60.38
1.6MPa Undisturbed	7	5.45	1009.07	0.99	1598.59	71.27
1.6MPa Undisturbed	8	5.45	1009.07	1.03	1599.26	82.17
1.6MPa Undisturbed	9	5.45	1020.61	1.06	1598.83	93.07
1.6MPa Undisturbed	10	5.45	1021.17	1.10	1600.11	103.96
0.4MPa Slurry	1	5.75	145.97	0.49	399.79	5.75
0.4MPa Slurry	2	5.75	155.23	1.03	399.79	17.04
0.4MPa Slurry	3	5.75	159.33	1.29	400.00	28.34
0.4MPa Slurry	4	5.75	162.38	1.47	399.89	39.64
0.4MPa Slurry	5	5.75	164.39	1.62	399.79	50.93
0.4MPa Slurry	6	5.75	165.27	1.75	399.68	62.23
0.4MPa Slurry	7	5.75	163.86	1.86	399.89	73.52
0.4MPa Slurry	8	5.75	164.85	1.96	399.89	84.82
0.4MPa Slurry	9	5.75	166.65	2.06	399.58	96.12
1.6MPa Slurry	10	5.75	166.12	2.15	399.68	107.41
1.6MPa Slurry	1	5.50	538.50	0.47	1599.89	5.50
1.6MPa Slurry	2	5.40	578.92	0.98	1599.89	16.09
1.6MPa Slurry	3	5.40	599.74	1.24	1600.11	26.59
1.6MPa Slurry	4	5.50	608.13	1.42	1600.32	37.09
1.6MPa Slurry	5	5.50	615.38	1.57	1600.11	47.49
1.6MPa Slurry	6	5.50	626.58	1.70	1599.58	57.89
1.6MPa Slurry	7	5.50	635.42	1.82	1599.79	68.28
1.6MPa Slurry	8	5.50	642.00	1.93	1599.47	78.58
1.6MPa Slurry	9	5.50	647.58	2.03	1599.58	88.88
1.6MPa Slurry	10	5.50	651.58	2.12	1599.36	99.18

Table S2. Magnetic susceptibility characteristics of the clay-rich materials from the Jin'nosuke-dani slip zone. High-field and low-field magnetic susceptibilities, the Khf/Klf ratio, and the inferred relative contribution of paramagnetic minerals are shown for the white clay and sheared black shale.

Sample	High field (m^3/kg)	Low field (m^3/kg)	High field / Low field	Paramagnetic faction (%)
White clay	8.95E-04	1.06E-03	8.46E-01	84.62
Black clay	1.31E-03	1.70E-03	7.67E-01	76.67